



**HAL**  
open science

## Effect of monotonic and cyclic temperature variations on the mechanical behavior of a compacted soil

Mojdeh Lahoori, Sandrine Rosin-Paumier, Farimah Masrouri

### ► To cite this version:

Mojdeh Lahoori, Sandrine Rosin-Paumier, Farimah Masrouri. Effect of monotonic and cyclic temperature variations on the mechanical behavior of a compacted soil. *Engineering Geology*, 2021, 290, pp.106195. 10.1016/j.enggeo.2021.106195 . hal-03512888

**HAL Id: hal-03512888**

**<https://hal.science/hal-03512888v1>**

Submitted on 13 Jun 2023

**HAL** is a multi-disciplinary open access archive for the deposit and dissemination of scientific research documents, whether they are published or not. The documents may come from teaching and research institutions in France or abroad, or from public or private research centers.

L'archive ouverte pluridisciplinaire **HAL**, est destinée au dépôt et à la diffusion de documents scientifiques de niveau recherche, publiés ou non, émanant des établissements d'enseignement et de recherche français ou étrangers, des laboratoires publics ou privés.



Distributed under a Creative Commons Attribution - NonCommercial 4.0 International License

# Effect of monotonic and cyclic temperature variations on the mechanical behavior of a compacted soil

Mojdeh Lahoori<sup>1</sup>, Sandrine Rosin-Paumier<sup>1</sup>, Farimah Masrouri<sup>1</sup>

mojdeh.Lahoori@univ-lorraine.fr

sandrine.rosin@univ-lorraine.fr

farimah.masrouri@univ-lorraine.fr

<sup>1</sup> *LEMTA-CNRS UMR 7563, Université de Lorraine, Vandoeuvre-lès-Nancy F-54500, France*

Corresponding author: Sandrine Rosin (email: sandrine.rosin@univ-lorraine.fr)

---

## Abstract

Settlement and slope stability of an embankment are mechanical aspects that play a major role in structural safety. Due to the tendency towards renewable energy, the embankments can be considered as a suitable medium for thermal energy storage. Using horizontal heat exchanger tubes, the thermal energy will be stored in different compacted soil layers in an embankment. Therefore, this structure can be subjected to daily and seasonally temperature variations due to heat extraction. Cyclic temperature variation can modify the mechanical behavior of compacted soils. Thus this study aims to investigate the effect of monotonic and temperature cycles in the range of 5 to 50 °C, on consolidation parameters and shear characteristics of a compacted sandy lean clay. To achieve this, temperature-controlled oedometric and direct shear tests were performed. Results showed that the effect of heating and cooling on mechanical properties is more pronounced under vertical stresses higher than the preconsolidation pressure. By heating, the normal consolidation line shifted to the left and consequently, the apparent preconsolidation decreased. Compression and swelling indexes could be considered independent of temperature variation. Due to the temperature cycles, the volumetric response of the compacted soil in oedometric and shear tests was stress history-dependent. Results of the direct shear tests showed that by temperature variation (heating/cooling and temperature cycles) the cohesion increased and the friction angle remained unchanged.

**Keywords:** Embankment, thermal energy storage, compacted soil, Thermo-Hydro-

30 Mechanical behavior, temperature-controlled oedometer tests, temperature-controlled di-  
31 rect shear tests.

## 32 **1 Introduction**

33 To limit the environmental impact of the production of needed energy, the energy geostruc-  
34 tures could provide new and clean solutions to the important issue of global warming for  
35 the years to come. These solutions still need to be further studied to provide appropriate  
36 techniques for both domestic and industrial energy needs.

37 Solar energy is an infinite, clean, and affordable source, it has a great potential to  
38 produce renewable thermal and electrical energy. Several technologies convert solar energy  
39 into a utilizable kind of energy for human needs like space heating. For example, solar  
40 energy storage consists of heat storage in a proper medium during summer to be preserved  
41 and later discharged for utilization in the winter (Stojanović and Akander 2010; Abedin  
42 and Rosen 2011). Several studies have demonstrated that the thermal energy storage in  
43 soils is a pertinent technique, due to their appropriate thermal properties and ease of  
44 access (Gan 2013; Beier and Holloway 2015).

45 In geotechnical engineering, different types of structures are made of compacted soils,  
46 such as roads and rail embankments. These linear structures contain several layers of  
47 compacted soils. To store the heat in an embankment in summer, and extract it in  
48 winter (or vice versa), the horizontal heat exchanger loops can be easily installed in these  
49 layers during the construction phase (Boukelia 2016; Jradi et al. 2017; Lahoori, Jannot,  
50 Rosin-Paumier, Boukelia and Masrouri 2020). For limited size embankments, in which  
51 the soil-atmosphere interaction during the charging and discharging season is high, the  
52 use of insulation material can be considered in design stage to avoid heat loss (Lahoori,  
53 Rosin-Paumier, Stoltz and Jannot 2020).

54 Generally, the soils and earthen structures are exposed to external daily and seasonally  
55 temperature variations. When the serviceability of these structures as thermal energy  
56 storage medium starts, they will be subjected in addition to internal seasonal temperature

57 variations. The temperature variation in soil storage mediums can fluctuate in the range  
58 of 10 to 50°C (Hesaraki et al. 2015). Variations in temperature have an impact on the  
59 volume of the constituents, which leads to changes in the deformability of the aggregates  
60 and the viscosity of the water. Thus, a heated material would be more deformable and  
61 the pore water would be less viscous and more mobile. However, this effect would be  
62 more or less important depending on the nature of soil constituents and its structure,  
63 inherited from the previous loading history (Cekerevac and Laloui 2004; Uchaipichat and  
64 Khalili 2009). This aspect is particularly important in the case of compacted soils. To  
65 prevent any damage, such as settlement and slope failure, and also to ensure the long-term  
66 structural stability of these energy structures, the effect of temperature variation on their  
67 mechanical behavior should be investigated.

68 Compacted soils are initially set up in an unsaturated state close to the saturation  
69 state (degree of saturation between 85 to 95%). During their service life and thermal  
70 exploitation in an embankment, the water content, the temperature and the applied  
71 mechanical loads are changing simultaneously.

72 Among different types of external loading, it is well known that landslides, settle-  
73 ments, and disorders of all kinds occur generally as a result of intense rainfall and seepage  
74 in embankments (Iverson and Major 1987; Rahardjo et al. 2001; Thibbotuwawa and  
75 Weerasekera 2013). Usually, the rainfall decreases the suction and increases the hydraulic  
76 conductivity in these unsaturated soils, this accelerates the soil saturation and the pore  
77 water pressure increase. As a result, the shear strength and factor of safety of the slope  
78 decrease (Rahardjo et al. 2001; Liu et al. 2017; Li et al. 2019).

79 Based on the aforementioned statements, this study focuses on investigating the thermo-  
80 hydro-mechanical behavior of compacted natural soil at saturated state, as in embank-  
81 ments, it is clearly the most critical state. For energy geostructures, a better understand-  
82 ing of the effect of monotonic and cyclic temperature variations on mechanical behavior  
83 such as consolidation and shear characteristics of compacted soil is of great importance.

84 Several researchers investigated the effect of temperature variations on consolidation  
85 and volumetric behavior of different types of soils under different stress paths (Tidfors and

86 Sällfors 1989; Eriksson 1989; Moritz 1995; Burghignoli et al. 2000; Cekerevac and Laloui  
87 2004; Uchaipichat and Khalili 2009; Di Donna and Laloui 2015). These investigations  
88 indicated that the effect of temperature on THM behavior of soils depends on the soil  
89 nature; the stress history and the thermal variation path.

90 Regarding the consolidation behavior, heated specimens exhibit a plastic behavior  
91 earlier compared to unheated ones, afterwards the elastic domain size reduces and shows a  
92 clear soil softening (Tidfors and Sällfors 1989). Thus, Thus, the apparent preconsolidation  
93 pressure ( $\sigma'_p$ ) decreases upon heating (Marques et al. 2004; Cekerevac and Laloui 2004).  
94 The effect of temperature variation on the compression and swelling indices ( $C_c$  and  $C_s$ )  
95 are found to be negligible in the temperature ranges from 20 to 90 °C (Cekerevac and  
96 Laloui 2004; Di Donna 2014).

97 In terms of volumetric behavior under temperature cycles, the soil initially in the  
98 normally consolidated state (NC) exhibits a contraction when temperature increases  
99 (Burghignoli et al. 2000; Cekerevac and Laloui 2004). However, different observations  
100 are reported during the following cooling. In some studies, cooling removes a small part  
101 of the thermal contraction caused by heating (Shetty et al. 2019), but in others, during  
102 cooling the thermal contraction continues to increase (Campanella and Mitchell 1968;  
103 Di Donna and Laloui 2015). Ma et al. (2017) reported that the thermal contraction  
104 becomes smaller after 4 or 5 successive heating and cooling cycles.

105 The soil in an overconsolidated state exhibits a thermal expansion during heating  
106 and with subsequent cooling, a reversible behavior is observed. Therefore, the thermal  
107 expansion with heating is dissipated (Di Donna and Laloui 2013; Shetty et al. 2019). This  
108 reversible behavior was observed with further heating and cooling cycles.

109 Based on most of the investigations that have focused on the study of the effect of  
110 temperature variations between 20 to 90 °C, it can be concluded that the preconsolidation  
111 pressure is a temperature dependent parameter and decreases with heating. But despite  
112 the importance of this parameter in thermal energy storage systems, its variations due to  
113 cooling and several heating-cooling cycles are poorly understood.

114 The other important mechanical characteristics of an energy structure such as a road

115 embankment are shear parameters: strength and stiffness, where the strength can be  
116 expressed in terms of apparent cohesion ( $c$ ) and friction angle ( $\varphi$ ). Although their de-  
117 pendency on temperature variations has been studied in recent years, the results are still  
118 controversial.

119 Cekerevac and Laloui (2004), using a temperature-controlled triaxial device in drained  
120 conditions for normally consolidated kaolin clay, have observed an increase of peak shear  
121 strength due to temperature increase while the critical state shear strength was indepen-  
122 dent of temperature. The same observation was reported by Abuel-Naga et al. (2007)  
123 for a normally consolidated soft Bangkok clay. Yavari et al. (2016), by performing direct  
124 shear tests, showed that for Fontainebleau sand and both normally and overconsolidated  
125 kaolin clay, the peak shear strengths were almost independent of temperature (5 to 40 °C).  
126 Maghsoodi et al. (2020) using a temperature controlled direct shear device, showed that  
127 the peak and critical shear strength of normally consolidated kaolin clay increased with  
128 a temperature increase from 22 to 60 °C, but no temperature dependence was observed  
129 for Fontainebleau sand.

130 The effect of temperature on friction angle ( $\varphi$ ) was reported to be negligible in several  
131 studies (Moritz 1995; Cekerevac and Laloui 2004; Maghsoodi et al. 2020). But there are  
132 different results for the cohesion ( $c$ ) variation upon heating and cooling cycles. Yavari  
133 (2014) found that the cohesion of a kaolin clay at three different temperatures (5, 20, and  
134 40 °C) is almost unchanged. On the contrary Maghsoodi et al. (2020) found that the  
135 temperature increase from 22 to 60 °C increased the cohesion for kaolin clay.

136 Regarding the mechanical loading cycles, Ng and Zhou (2014) using a temperature  
137 controlled device reported that the axial plastic strain accumulated during cyclic load-  
138 ing-unloading is larger at higher temperatures for a silty soil. Very few studies have  
139 investigated the impact of thermal cycles on shear characteristics. For example, Yazdani  
140 et al. (2019) have investigated the effect of temperature cycles on shear characteristics.  
141 Their study is mostly focused on soil-structure interface mechanical behavior. There-  
142 fore, the effect of several temperature cycles on the shear behavior of soils needs to be  
143 investigated.

144 The shear characteristics evolution due to the monotonic and cyclic temperature vari-  
145 ations depends on several parameters such as material characteristics and soil nature,  
146 overconsolidation ratio, experimental conditions, and thermo-mechanical paths. But the  
147 results are not numerous enough, and there are still many unanswered questions on this  
148 subject.

149 This experimental study aims to investigate the thermo-mechanical behavior of a com-  
150 pacted sandy lean clay that is currently used in embankment constructions, in the sat-  
151 urated state under different stress paths. Temperature-controlled oedometer and direct  
152 shear devices were used to perform consolidation and shear tests under monotonic and  
153 cyclic temperature variations. The main aspects of the thermo-mechanical behavior of  
154 the compacted soil that are tackled in this study are to investigate the effect of cooling  
155 (20 to 5 °C), heating (20 to 50 °C), and thermal cycles (5-50 °C) on consolidation and  
156 shear characteristics.

## 157 **2 Soil properties, devices, and specimen preparation**

### 158 **2.1 Soil properties**

159 The tested soil was extracted from the Paris region in France. X-ray diffractograms  
160 analysis reveals that it contains 81% quartz, 7% dolomite, 5% calcite, 5% clayey materials,  
161 and 3% feldspar (Boukelia 2016). This material was dried, pulverized, and sieved through  
162 a 2 mm sieve before being used for various experiments. According to the particle-size  
163 distribution tests, almost 20% of the particles of the soil were smaller than 2 μm, and 41%  
164 were smaller than 80 μm (Figure 1). With a liquid limit (LL) of 27% and a plastic limit  
165 (PL) of 21%, the plasticity index (PI) was 6% (AFNOR 1993). The standard Proctor  
166 test results showed an optimum water content ( $w_{opt}$ ) of 16% and a maximum dry density  
167 ( $\rho_d$ ) of 1.81 Mg.m<sup>-3</sup> (Table 1).

168

169 The material was classified as sandy lean clay, CL, according to the Unified Soil Clas-  
170 sification System (ASTM 2000). In this study, the soil specimens were prepared at a

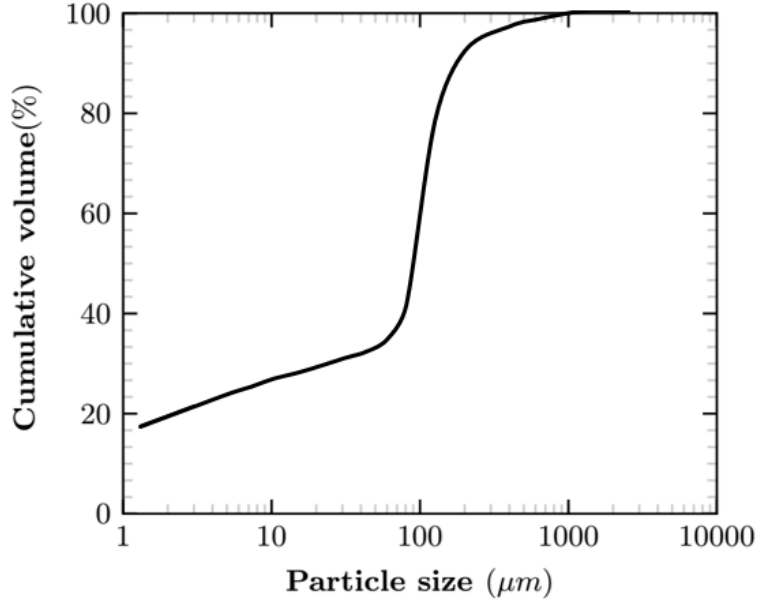


Figure 1: Particle size distribution (Boukelia 2016)

Table 1: Characteristics of the studied soil

Properties	Amount
Plasticity limit (%)	20.5
Liquidity limit (%)	27.2
Plasticity index (%)	6.6
$w_{opt}$ (%)	16.1
$\rho_d$ ( $Mg/m^3$ )	1.8
Class of soil	CL
Thermal conductivity (W/m.K)	2.46
Volumetric heat capacity ( $J/k.m^3$ )	2.64
Thermal diffusivity ( $m^2/s$ )	$9.6 \times 10^{-7}$

171 water content ( $w$ ) of 16.3 % and a dry density  $\rho_d$  of  $1.79 Mg.m^{-3}$  in accordance with the  
 172 optimal thermal condition defined by Boukelia (2016). The dry soil was wetted up to the  
 173 desired water content by adding the distilled water and stored in plastic bags for almost  
 174 3 days before being compacted in the cells for each test.

## 175 2.2 Device and specimen preparation: oedometric tests

176 A temperature-controlled oedometric device was used to investigate the effect of temper-  
 177 ature on the consolidation behavior of the studied compacted soil. The system included  
 178 a cylindrical cell of stainless steel (70 mm in diameter) and a piston to apply the vertical  
 179 stress using a load frame (Figure 2). The vertical deformation of the specimen was mea-  
 180 sured using a linear variable differential transducer (LVDT) with an accuracy of  $10^{-5}$  m.



181 To impose the desired temperature, a heating-cooling device circulated fluid in the spiral  
 182 tubes around the soil specimen, and a K-type thermocouple was placed in the bottom  
 183 part of the oedometer cell to measure the temperature of the specimen during the tests.  
 184 The system comprised also a volume/pressure controller to control the pore water pres-  
 185 sure at the base of the specimen. To minimize the thermal losses, the oedometric cell was  
 186 insulated with a polystyrene box. To maintain a constantly saturated state during tests,  
 187 a continuous water supply was maintained.

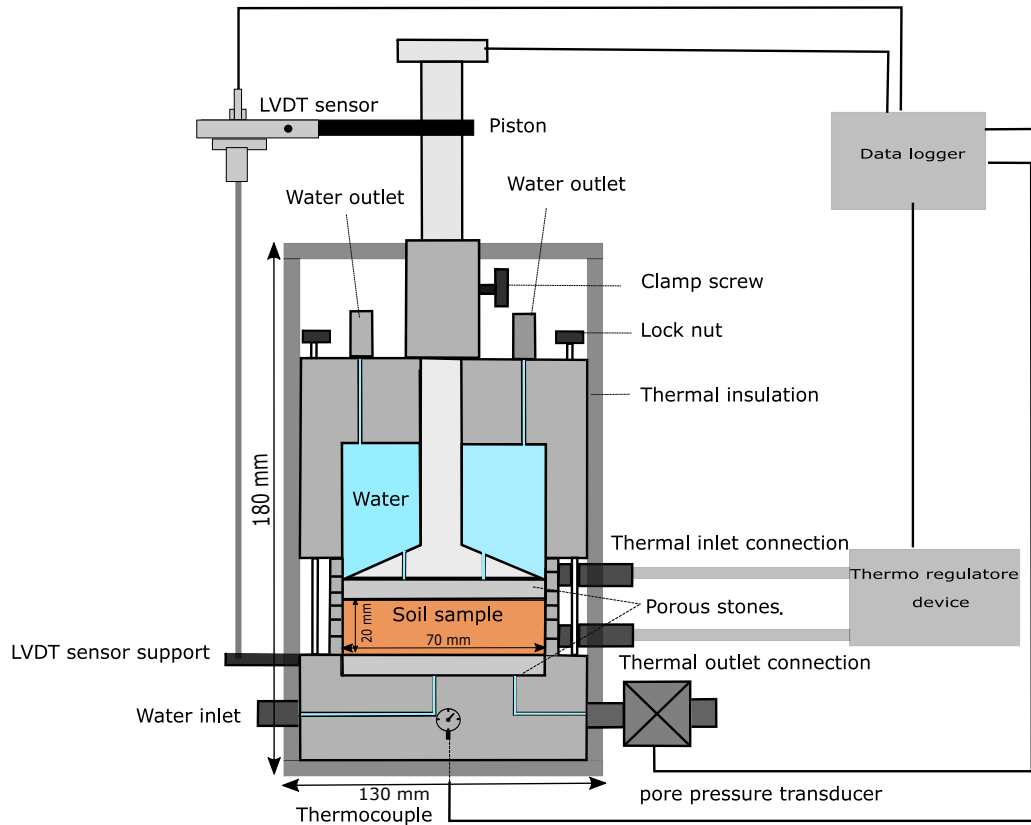


Figure 2: Temperature-controlled oedometer device.

188 Thermal calibration was performed to take into account the effect of temperature on  
 189 different parts of the device and corrections were applied to the results. The thermal  
 190 deformation of the oedometric cell was observed by measuring the vertical displacement  
 191 of the piston during cycles of heating and cooling under 10 kPa of vertical stress. The  
 192 device was first heated from 20 °C to 50 °C, and then was cooled up to 5 °C and finally  
 193 was heated up to 20 °C in steps of 10 °C. Figure 3 shows the relationship between  
 194 the measured thermal vertical displacement ( $\Delta h_T$ ) of the oedometric cell using LVDT at

195 different applied temperatures. The heating caused dilation in the oedometric cell, while  
 196 cooling caused a contraction. A linear equation can be determined as follows:

$$\Delta h_T = -0.0026\Delta T + 0.05 \quad (1)$$

197 Where  $\Delta T$  is temperature variation ( $^{\circ}C$ ).

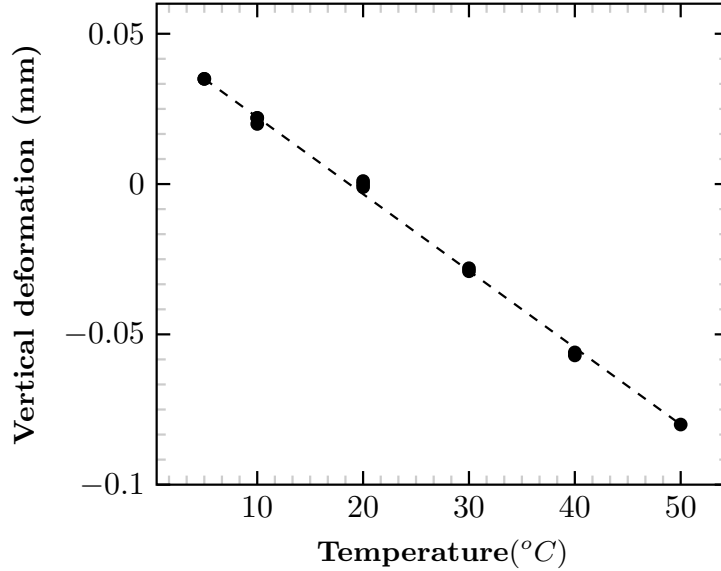


Figure 3: Thermal calibration of temperature-controlled oedometric device.

198 The abovementioned relationship was used to correct the measurements of the sample  
 199 deformation during temperature variations by following equation:

$$\Delta h_{T(sample)} = \Delta h_{T(sample+cell)} - \Delta h_{T(cell)} \quad (2)$$

200 where  $\Delta h_{T(sample+cell)}$  is the measured total displacement during heating or cooling  
 201 phases.

202 To perform oedometric tests, the soil at the water content 16.3 % was compacted  
 203 directly in the oedometric cell (70 mm in diameter and 20 mm in height) to reach the  
 204 target dry density of  $1.79 Mg.m^{-3}$ . Then, the saturation phase was started by applying  
 205 a backwater pressure of 9 kPa through the bottom part of the oedometric cell (through  
 206 the water inlet, in Figure 2). The saturation phase was performed at 20  $^{\circ}C$  under 9 kPa  
 207 of vertical stress. To check the saturation state, the hydraulic conductivity was measured

208 over a long time (7 days) to achieve an equilibrium state, and also the water content of  
 209 several samples was measured after several days. Afterward, different thermo-mechanical  
 210 paths were applied, they are presented in detail in section 3.1.

### 211 2.3 Device and specimen preparation: direct shear tests

212 The temperature-controlled direct shear device contains a shear box (60 x 60 x 30 mm)  
 213 that is placed inside a container filled with water to maintain the saturation state of the  
 214 samples (Figure 4). The heating-cooling system circulates fluid at the desired temperature  
 215 under the container. The temperature is checked using 3 different thermocouples placed:  
 216 in the upper half of the shear box; in the lower half of the shear box and the container.  
 217 A piston applies the normal stress  $\sigma_n$  (kPa) on the top of the soil specimen using a load  
 218 frame. The shear displacement and the normal displacement were measured using two  
 219 linear variable differential transducers (LVDT) (Figure 4). To obtain the real volume  
 220 change of the soil sample, the thermal calibration of the different parts of the device was  
 221 performed.

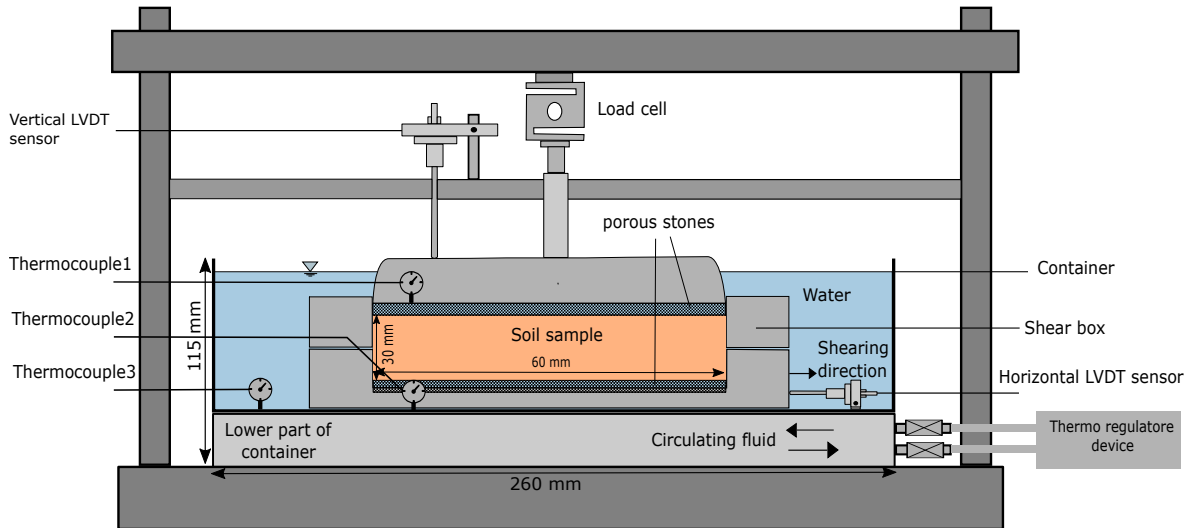


Figure 4: Temperature-controlled direct shear device.

222 Before direct shear tests, the soil at the initial water content (16.3 %) was compacted  
 223 directly in the shear box at the density of  $1.79 \text{ Mg.m}^{-3}$ . The specimens were saturated  
 224 by leaving them inside a water container at  $20 \text{ }^\circ\text{C}$ . The saturation level was checked by  
 225 measuring the water content of different specimens after several days. After one week, the

226 measured water content was close to the estimated water content of a saturation state.  
227 This duration was repeated for all the samples.

## 228 **3 Experimental programs**

229 The experimental programs to take into account the effect of cooling (20 to 5 °C), heating  
230 (20 to 50 °C), and several heating-cooling cycles in the range of 5 to 50 °C on consolidation  
231 and shear behavior are presented in the following.

### 232 **3.1 Consolidation program**

#### 233 **3.1.1 Monotonic thermo-mechanical paths**

234 Standard oedometric tests were conducted at different temperatures to investigate the  
235 effect of temperature on the consolidation parameters as compression index ( $C_c$ ), swelling  
236 index ( $C_s$ ), and apparent preconsolidation pressure ( $\sigma'_p$ ). After the saturation phase, one  
237 reference standard oedometric test at 20 °C was performed (test number 1 in Table 2).  
238 The specimen was loaded by applying successive vertical stress increments in different  
239 steps in the range of 9 to 1600 kPa and then was unloaded to 100 kPa. From ASTM  
240 (2011), each step took 24 hours, and from t90 of settlement versus time curves, the end  
241 of consolidation was determined. For oedometric tests at different temperatures, the soil  
242 specimen was cooled from 20 to 5 °C or heated up from 20 to 50 °C with a heating/cooling  
243 rate of 5 °C/h after the saturation phase. The heating/cooling rate was sufficiently slow to  
244 avoid excess pore water pressure generation due to the temperature variation (Cekerevac  
245 and Laloui 2004; Shetty et al. 2019). Then the complete oedometric tests were performed  
246 (tests number 2-3 in Table 2).

247

#### 248 **3.1.2 Cyclic thermo-mechanical paths**

249 The tests numbers 4 to 7 in Table 2 were supposed to reproduce the volumetric response  
250 of compacted soil element in different depths of an embankment which is under internal

Table 2: Experimental programme for consolidation tests (*L*=loading, *U*=unloading, *C*=cooling, *H*=heating and *TC* = thermal cycles).

Test number	Test type	Temperature ( $^{\circ}C$ )	Vertical effective stress (kPa)	OCR before TC	TC ( $^{\circ}C$ )
1	L-U	20	9-1600-100	-	-
2	C-L-U	5	9-1600-100	-	-
3	H-L-U	50	9-1600-100	-	-
4	L-4 TC	20	9	8	5-50
5	L-4 TC	20	9-170	1	5-50
6	L-4 TC	20	9-400	1	20-50
7	L-U-4 TC	20	9-1600-100	16	20-50

251 and external seasonal temperature variations.

252 Therefore, to simulate the effect of external seasonal temperature variation due to  
 253 the soil-atmosphere interaction, compacted soil sample in test number 4 (Table 2) was  
 254 subjected to 4 temperature cycles in the range of 5 to 50  $^{\circ}C$  after saturation phase under  
 255 9 kPa. The thermal load (heating and cooling) was applied by successive increments of  
 256  $\Delta T=10$   $^{\circ}C$  (5  $^{\circ}C/h$ ).

257 The test numbers 5 to 7 consider the effect of internal temperature variation due to  
 258 the heat transfer from a horizontal heat exchanger that is commonly horizontal installed  
 259 at 2m from the base. Considering 10m height embankment, the total vertical stress is 170  
 260 kPa ( $20.8 \text{ kN.m}^{-3} \times 8 \text{ m}$ ). Therefore, test number 5 (Table 2) was thus done by applying  
 261 the vertical stress from 9 to 170 kPa, and then 4 temperature cycles (5 to 50  $^{\circ}C$  ) were  
 262 applied. Besides these conditions, during the lifetime of the embankment, the compacted  
 263 soil may be loaded or unloaded. Test number 6 (Table 2) simulated a subsequent loading  
 264 of the compacted soil. Therefore, the soil sample was vertically loaded from 9 to 400 kPa  
 265 and then 4 temperature cycles (20 to 50  $^{\circ}C$ ) were applied (test number 6 in Table 2). To  
 266 reach a highly overconsolidation state (OCR=16) four temperature cycles in the range  
 267 of 20 to 50  $^{\circ}C$  were applied after a loading (1600 kPa) and unloading of 100 kPa (test  
 268 number 7 in table 2).

## 3.2 Direct shear program

### 3.2.1 Monotonic thermo-mechanical paths

The direct shear tests at different temperatures were conducted to investigate the effect of the cooling and heating on shear parameters. After the saturation phase at 20 °C, the normal stress was applied to the compacted soil (paths 0 – 1 in Figure 5). Three values of initial normal stresses ( $\sigma'_n=50, 100, 200$  kPa) were chosen. These values correspond to the soil pressure in the depths of 2.5 m, 5 m, and 10 m in an embankment assuming a density of  $20.8 \text{ kN.m}^{-3}$ . After the consolidation phase, the shear test at 20 °C was done (paths 1 – 2 in Figure 5, tests 1-3, Table 3). From the settlement curve and the time required for the specimen to achieve 50 percent of its consolidation under the maximum normal stress ( $t_{50}$ ) a shearing rate of  $0.02 \text{ mm.min}^{-1}$  was calculated (ASTM 1994). This slow rate applied for the shear test was supposed to ensure drained conditions during shearing. To take into account the effect of temperature variation on shear parameters, after the consolidation phase, the cooling or heating phase was applied (paths 1 – 1' and 1 – 1'' in Figure 5). Finally, when the soil volumetric variation stabilized, the specimens were sheared with a rate of  $0.02 \text{ mm.min}^{-1}$  (paths 1' – 2' and 1'' – 2'' in Figure 5, tests 4-10, Table 3).

### 3.2.2 Cyclic thermo-mechanical paths

The thermal cycles under constant normal stress were performed on compacted soil specimens in the direct shear box to evaluate the variation of shear parameters (cohesion and friction angle) after the thermal cycles. As the monotonic thermo-mechanical path, after the saturation phase at 20 °C, three normal stresses ( $\sigma'_n=50, 100, 200$  kPa) were applied on different compacted soil specimens at 20 °C. After the consolidation phase, 5 thermal cycles in the range of 5 to 50 °C were applied by a successive increment of  $\Delta T=10$  °C (5 °C/h). After thermal cycles, when the thermal volume change stabilized, the specimens were sheared at 20 °C with a displacement rate of  $0.02 \text{ mm.min}^{-1}$  (tests 11 to 13, Table 3).

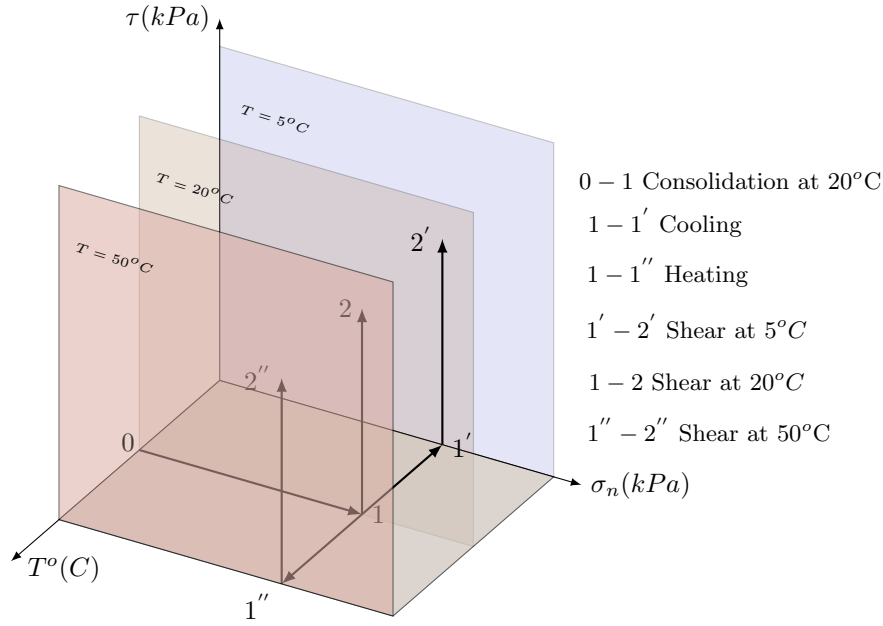


Figure 5: Thermo-mechanical path for direct shear tests at different temperatures.

296

## 297 4 Experimental results

298 This part presents the results from oedometric and direct shear tests under different  
 299 thermo-mechanical paths. The following part will be dedicated to the scientific discussion.

### 300 4.1 Thermo-mechanical results for oedometric tests

#### 301 4.1.1 Monotonic thermo-mechanical oedometric results

302 Three standard oedometric tests at different temperatures were carried out (5, 20, and  
 303 50°C). The void ratios for all of the specimens after saturation remained unchanged  
 304 due to the zero swelling potential of this compacted soil. The void ratio variations after  
 305 cooling and heating were negligible.

306 Figures 6a and b show the normalized settlement and void ratio variations against  
 307 the vertical effective stresses at different temperatures respectively. The results show  
 308 that, with temperature increase at vertical stresses higher than 100 kPa, the vertical  
 309 displacement increased, and at the same time the void ratio decreased (Figure 6b). These

Table 3: Experimental programme for direct shear test (TC=thermal cycles)

Test number	Density (Mg/m <sup>3</sup> )	Type	Temperature °C	effective normal stress (kPa)
1	1.77	Loading-Shearing	20	50
2	1.76	Loading-Shearing	20	100
3	1.76	Loading-Shearing	20	200
4	1.75	Loading-Cooling-Shearing	5	50
5	1.76	Loading-Cooling-Shearing	5	100
6	1.77	Loading-Cooling-Shearing	5	100
7	1.76	Loading-Cooling-Shearing	5	200
8	1.75	Loading-Heating-Shearing	50	50
9	1.77	Loading-Heating-Shearing	50	100
10	1.76	Loading-Heating-Shearing	50	200
11	1.78	Loading-5 TC-Shearing	20 (5-50)	50
12	1.78	Loading-5 TC-Shearing	20 (5-50)	100
13	1.78	Loading-5 TC-Shearing	20 (5-50)	200

310 results show that the heated soil becomes more compressible and the soil capability to  
311 support a vertical stress decreases, as a consequence the normal consolidation line moves  
312 to the left. Therefore, for the studied soil, the consolidation behavior could be considered  
313 as temperature-dependent and with temperature increase, a thermal softening could be  
314 expected.

Table 4: Consolidation parameters of studied soil at different temperatures.

Temperature °C	Initial void ratio	$C_c$	$C_s$ (unloading)	$\sigma'_p$ (kPa)
5	0.516	0.035	0.01	80
20	0.517	0.037	0.01	75
50	0.518	0.040	0.013	65

315

316 From the results obtained in standard oedometric tests at different temperatures  
317 (Figure 6b), the slope of the normal compression lines defined as compression index  
318 ( $C_c = \Delta e / \Delta \log \sigma'_v$ ), and the slope of the unloading lines defined as a swelling index  
319 ( $C_s = \Delta e / \Delta \log \sigma'_v$ ) were obtained and are presented in the Table 4. The results showed  
320 that their variation with temperature appears as they changed very slightly with temper-  
321 ature variation.

322 The apparent preconsolidation pressure  $\sigma'_p$  was evaluated using the Casagrande method  
323 (Casagrande 1936) for each standard oedometric curves at each temperatures (5, 20, 50



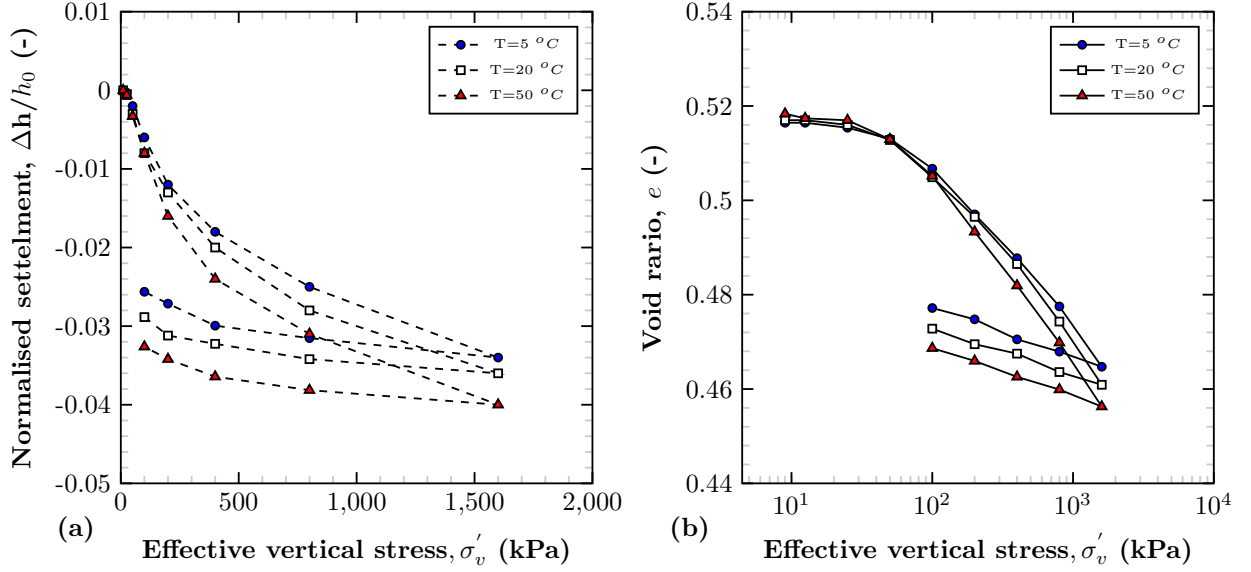


Figure 6: (a) normalized settlement and (b) void ratio variations against effective vertical stress at different temperatures.

324 °C). The results presented in Table 4. The preconsolidation pressure  $\sigma'_p$  reached 80, 75,  
 325 and 65 kPa at 5, 20 to 50 °C respectively.

326 From the results of void ratio variations against vertical stress the hydraulic conduc-  
 327 tivity was calculated for each load increment at different temperatures using the following  
 328 equation:

$$k = C_v m_v \gamma_w \quad (3)$$

329 where  $k$  is the hydraulic conductivity ( $m.s^{-1}$ ),  $C_v$  is the coefficient of consolidation  
 330 ( $m^2.s^{-1}$ ),  $m_v$  is the coefficient of volume compressibility ( $kPa^{-1}$ ) and  $\gamma_w$  is the unit  
 331 weight of water at a given temperature ( $kN.m^{-3}$ ).

332 The hydraulic conductivity as function of void ratio is shown in Figure 7 (a). Figure  
 333 7(a) shows that when the void ratio decreased, the hydraulic conductivity decreased due  
 334 to the increasing density. For example, in Figure 7(a), under 1600 kPa of vertical stress,  
 335 the hydraulic conductivity increased as temperature increases whereas the void ratio de-  
 336 creased. Delage et al. (2009) observed the same trend for hydraulic conductivity of Boom  
 337 clay under different temperatures. They pointed out that these results may be due to  
 338 the coupled effect of changes in water properties and porosity due to the temperature  
 339 variation. However, Morin and Silva (1984) and Abuel-Naga et al. (2005) reported that

340 the impact of soil volume change due to the temperature variation is too small to be con-  
 341 sidered as a reason for the change of hydraulic conductivity at elevated temperature (90  
 342 °C). With temperature increase, the viscosity of water decreases and leads to an increase  
 343 in the soil hydraulic conductivity (Hillel 1980) therefore the water flows are more freely  
 344 through the porous network.

345 Based on the hydraulic conductivity test results at different temperatures, an equation  
 346 is proposed to determine the intrinsic permeability  $K$  ( $m^2$ ):

$$k = \frac{K\gamma_w(T)}{\mu(T)} \quad (4)$$

347 where  $k$  is the hydraulic conductivity ( $m.s^{-1}$ ),  $\gamma_w$  is the unit weight of water ( $kN.m^{-3}$ ),  $\mu$   
 348 is the water viscosity ( $Pa.s$ ) and  $T$  is the temperature ( $K$ ). According to the literature,  
 349 the viscosity of water in effective porosity decreases at higher temperature:

$$\mu(T) = -0.00046575Ln(T) + 0.00239138 \quad (5)$$

350 Figure 7 (b) shows the variation of intrinsic permeability against the void ratio. Based  
 351 on this figure a linear relationship was evidenced between the intrinsic permeability and  
 352 the void ratio variations. These results were in agreement with the study of Li et al.  
 353 (2018) on intact and remolded sensitive clay and with the study of Delage et al. (2009)  
 354 on Boom clay. Therefore, the temperature dependence of water viscosity could partly  
 355 explain the hydraulic conductivity variations upon thermal solicitations.

#### 356 4.1.2 Thermal cycles effect on the volumetric variation of studied compacted soil

357 The results of volumetric variation against temperature cycles under 9 kPa are presented in  
 358 Figure 8a (test number 4, Table 2). With heating from 20 to 50 °C the volumetric response  
 359 was almost negligible whereas, during cooling from 50 to 5 °C the sample dilated slightly.  
 360 With further temperature cycles, the soil specimen showed a thermo-elastic response and  
 361 the volumetric variations were reversible. This reversible behavior corresponds to the  
 362 thermo-elastic expansion and contraction of the solid skeleton.

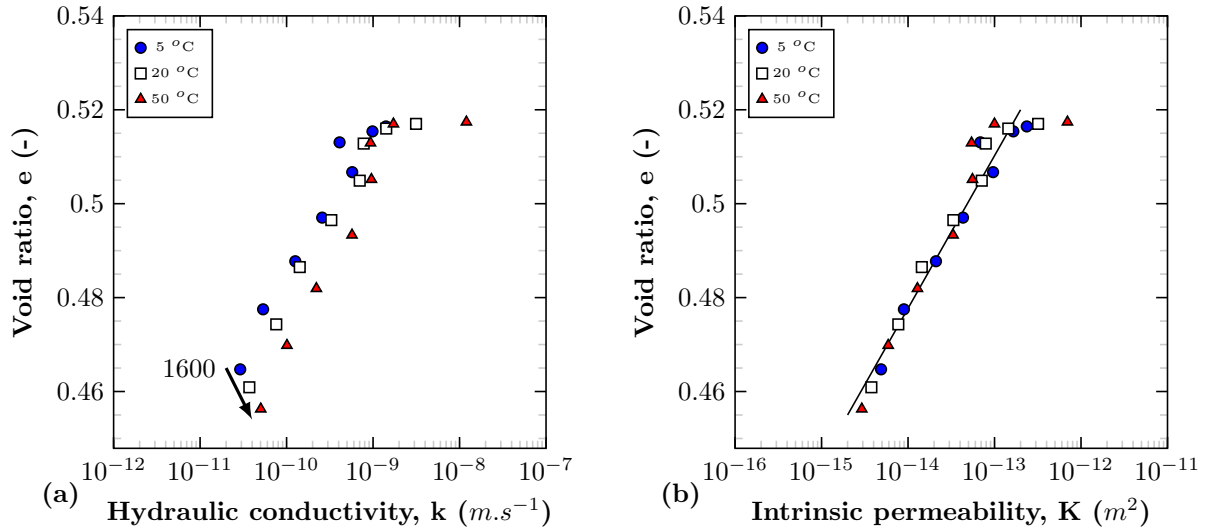


Figure 7: Effect of the temperature on (a) hydraulic conductivity ( $k$ ) and (b) intrinsic permeability ( $K$ ).

363 Under 170 kPa the soil was in normally consolidated condition (void ratio after tem-  
 364 perature cycles=0.5) and after first heating (20 to 50 °C), the specimen contracted as  
 365 a volume decrease of 0.13% was observed (Figure 8a). To determine the elastic or plas-  
 366 tic nature of thermal loading, after heating, the sample is cooled down to 5 °C and the  
 367 volume of the specimen slightly decreased (0.17%). The volume variations during the  
 368 first thermal cycle (20-50-5 °C) were irreversible. But this thermal contraction decreased  
 369 cycle by cycle and after four thermal cycles, the deformation was stabilized and an elastic  
 370 behavior was reached. In Figure 8a, it appears that the part of the curve under 20 °C is  
 371 superimposed. In the following, the temperature cycles were applied in the range of 20 to  
 372 50 °C.

373 After thermally induced volume changes verification for effective in-situ stress states,  
 374 two extreme cases were applied. In test number 6 under 400 kPa (NC state, void ratio  
 375 after temperature cycles=0.48), 4 thermal cycles (20 to 50 °C) exhibited a thermal plastic  
 376 contraction increasing when the number of thermal cycles increased (Figure 8b). In highly  
 377 OC state (OCR=16) in test number 7 (Table 2), again 4 thermal cycles in the range of 20  
 378 to 50 °C were applied. In this state, after a slight deformation, the soil specimen showed  
 379 a reversible volumetric response (Figure 8b).

380 The elastoplastic deformation due to the thermal cycles at OC (at 9 kPa) and NC (at  
 381 170 and 400 kPa) states leads to a void ratio variation at constant vertical stress. To

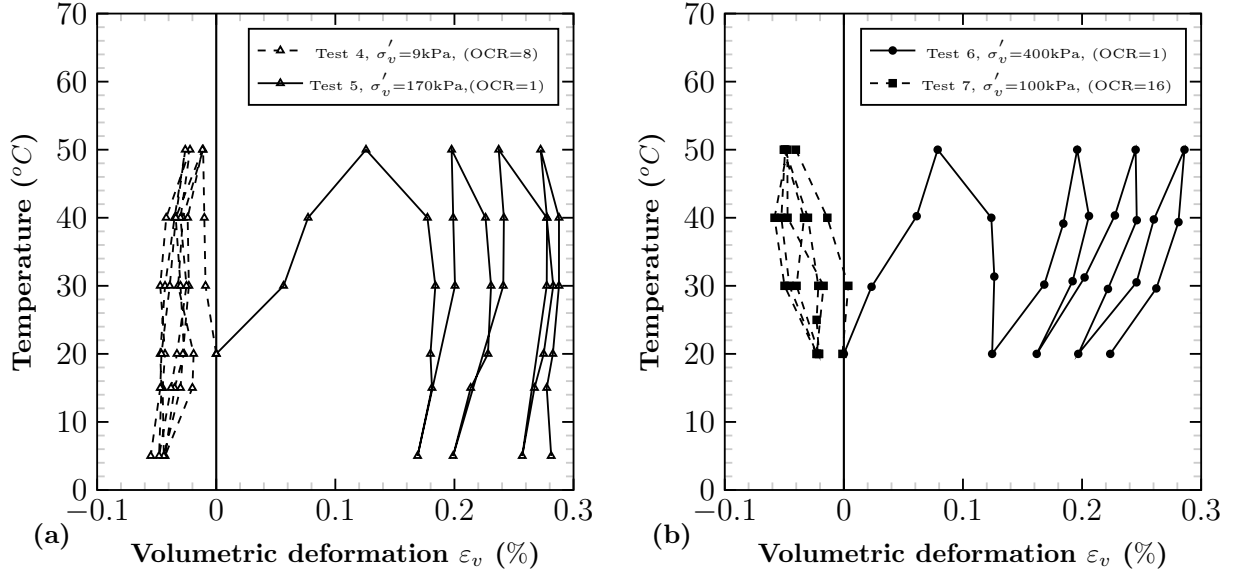


Figure 8: Volumetric deformation during thermal cycles under a) 9 kPa (test 4,  $\text{OCR}=8$ ) and 170 kPa (test 5,  $\text{OCR}=1$ ) b) 400 kPa (test 6,  $\text{OCR}=1$ ) and 100 kPa (test 7,  $\text{OCR}=16$ )

382 compare the effect of thermal cycles on soil with a reference oedometric test at 20 °C,  
 383 the evolution of normalized void ratios versus effective vertical stress for both types of  
 384 tests with thermal cycles and reference oedometric tests, are depicted in Figure 9. Figure  
 385 9a shows that the void ratio increased after the thermal cycles under 9 kPa (OC state).  
 386 To detect the effect of this variation on the subsequent loading, the specimen was then  
 387 loaded vertically. The whole curve is slightly higher than the reference test (black points).  
 388 The slope of the consolidation line ( $C_c=0.036$ ) was the same as the reference test, and  
 389 the temperature cycles had a negligible effect on the apparent preconsolidation pressure.

390 Figure 9b and 9c show the void ratio variations for applied thermal cycles under 170  
 391 and 400 kPa respectively (test 5 and 6, Table 2). The void ratios, before applying thermal  
 392 cycles, coincided with the reference oedometric test at 20 °C. After thermal cycles, the  
 393 void ratio in NC state decreased for both tests. These variations are due to the thermally  
 394 induced plastic deformation that can be considered as a thermal hardening. These void  
 395 ratios corresponded to a void ratio in higher vertical stress for the reference test at 20 °C.  
 396 For instance, in Figure 9b the normalized void ratio after thermal cycles under 170 kPa  
 397 was 0.95 which corresponds to vertical stress of 230 kPa for the reference test at 20 °C  
 398 (blue point in Figure 9b). Therefore, when the specimen is subjected to thermal cycles

399 it behaves like an over-consolidated soil. After this loading, the specimens were loaded  
400 vertically and the void ratios for both tests reached the same void ratio as the reference  
401 test. The slope of the subsequent loading line after thermal cycles (slope of ac line in  
402 Figure 9b) is 0.021 while the slope for the normal consolidation line at 20 °C is 0.037.

## 403 **4.2 Thermo-mechanical results for direct shear test**

### 404 **4.2.1 Monotonic thermo-mechanical direct shear results**

405 In this section, the effect of cooling and heating on shear characteristics is investigated.  
406 In temperature-controlled direct shear tests, after the saturation phase, the consolida-  
407 tion phase was started and the specimen was loaded vertically at three different normal  
408 stresses  $\sigma'_n=50, 100, \text{ and } 200$  kPa at 20 °C. After this consolidation phase, a heating  
409 or cooling phase (5 °C/h), was applied to the compacted soil specimens. The cooling  
410 phase was conducted from 20 to 5 °C and the heating phase from 20 to 50 °C. The re-  
411 sults showed that the cooling phase had a negligible effect on the volumetric deformation  
412 of the specimens whereas during heating, the specimens contracted and the volumes of  
413 the specimens decreased slightly. Figure 10a shows the volumetric deformation due to the  
414 thermal softening of the samples in the shear box. The volume of the specimens decreased  
415 by 0.07, 0.12, and 0.14 % for the normal stresses of 50, 100, and 200 kPa respectively.

416 When the thermal volumetric deformation stabilized, the compacted soil was sheared  
417 with a rate of 0.02 mm/min. Figure 11 shows the variation of the shear strength against  
418 shear displacement for  $\sigma'_n=50, 100, \text{ and } 200$  kPa at 5, 20, and 50 °C. To ensure the  
419 quality of the results, several tests were duplicated, for example, the test under  $\sigma'_n=100$   
420 kPa at 5 °C (Figure 11b). Under normal effective stress of 50 kPa and 100 kPa, the shear  
421 strengths were not affected by heating or cooling (Figure 11a). However, the heated and  
422 cooled specimens showed a higher dilatation than the specimen at 20 °C (Figure 11d).  
423 Under 200 kPa, the shear stress was not affected by heating whereas cooling reduced it by  
424 9 % (Figure 11c). For these samples during shearing, the soil specimen slightly contracted  
425 at first, then this contraction was followed by a negligible dilatation (Figure 11f).

426 To obtain the shear characteristics (cohesion,  $c$  and friction angle  $\varphi$ ), the shear stress

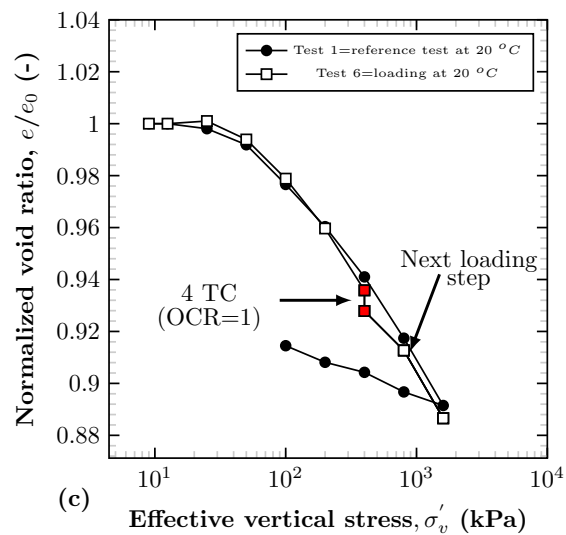
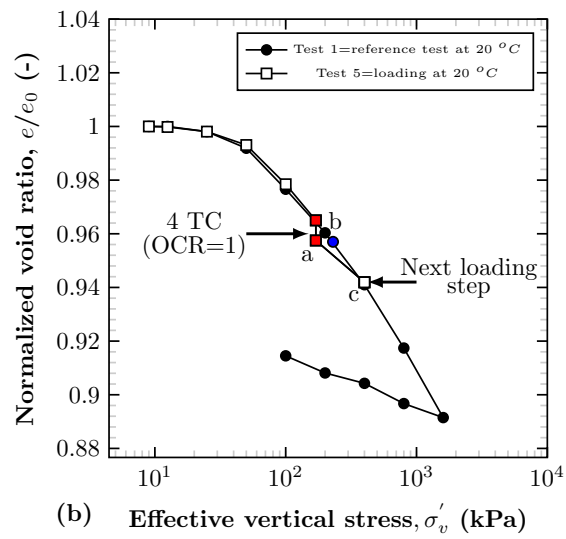
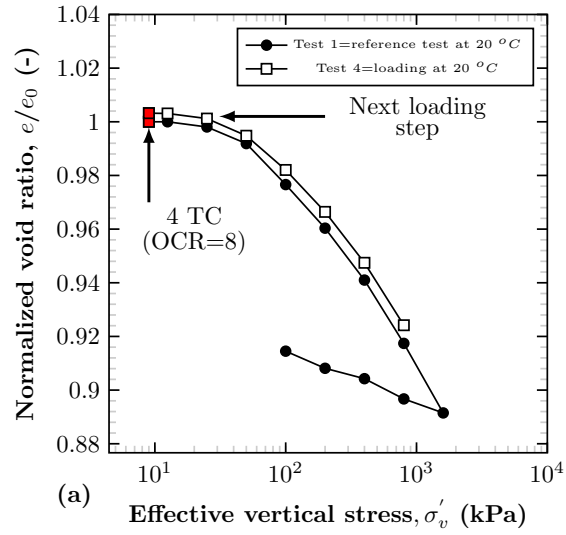


Figure 9: Void ratios variation after thermal cycles under (a) 9 kPa (b) 170 kPa (b) 400 kPa, TC=temperature cycles.

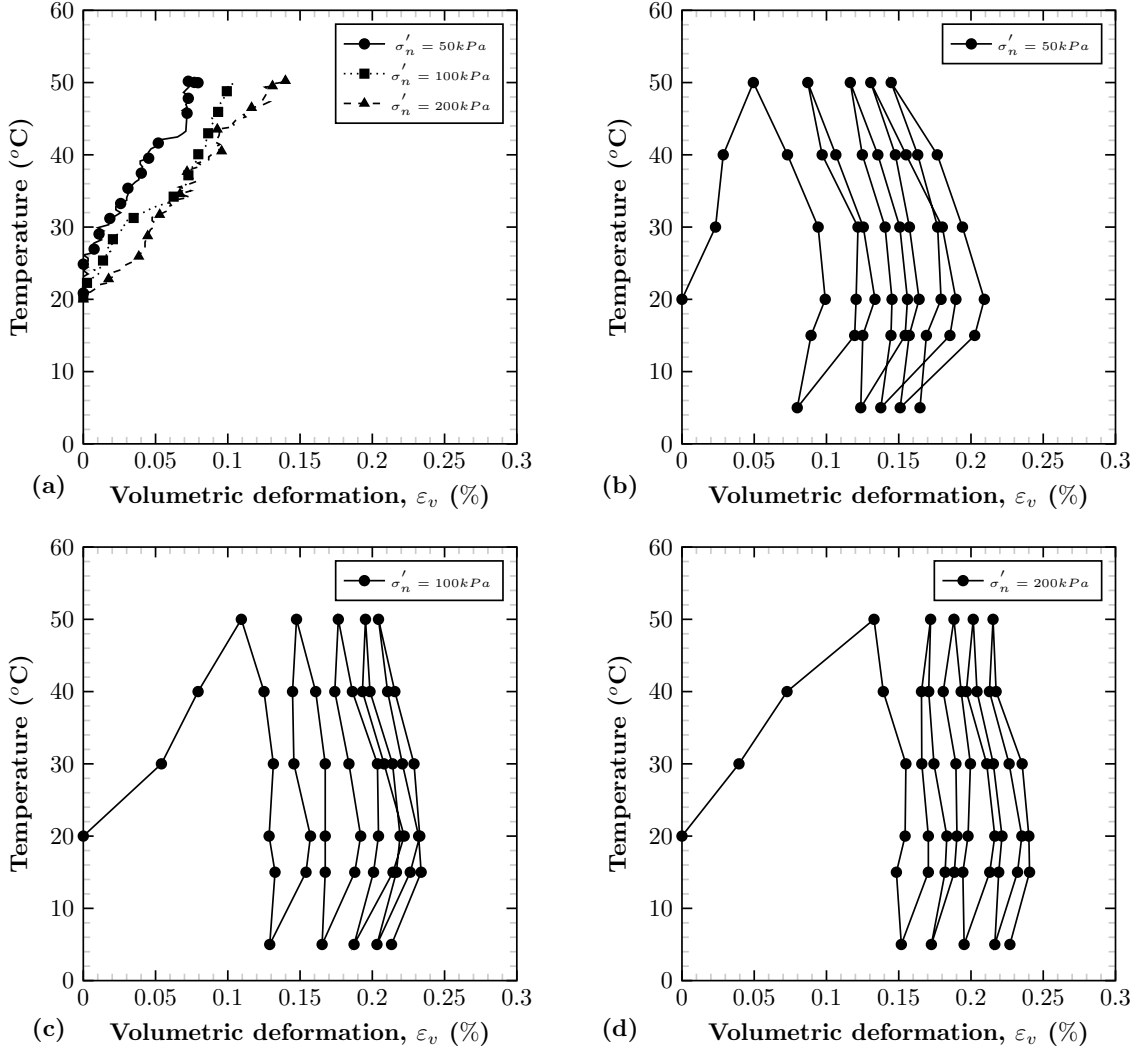


Figure 10: Thermal volumetric deformation (a) during heating from 20 to 50 °C (b), (c) and (d) during 5 thermal cycles at  $\sigma'_n = 50, 100$  and  $200$  kPa respectively.

427 corresponding to 10 % of the sample length was taken for each test and is presented in  
 428 Table 5. Figure 12 shows the Mohr-Coulomb plane for the studied soil at different temper-  
 429 atures. The results show that cooling ( $\Delta T = -15^\circ C$ ) changed the shear characteristics:  
 430 the cohesion increased from 13.0 to 20.5 kPa and the friction angles decreased slightly  
 431 from  $34.4^\circ$  to  $30.5^\circ$ . The heating ( $\Delta T = +30^\circ C$ ) increased slightly the cohesion by 4 kPa  
 432 (from 13.0 to 17.4 kPa) and the friction angle was not affected.

433 It can be concluded that the thermal volumetric deformation during heating did not  
 434 affect the shear strength but cooling decreased it and this behavior was more pronounced  
 435 under high normal stresses. Regarding the volumetric variation during the shear phase,  
 436 at low normal effective stresses, the compacted soil tended to dilate. However, with

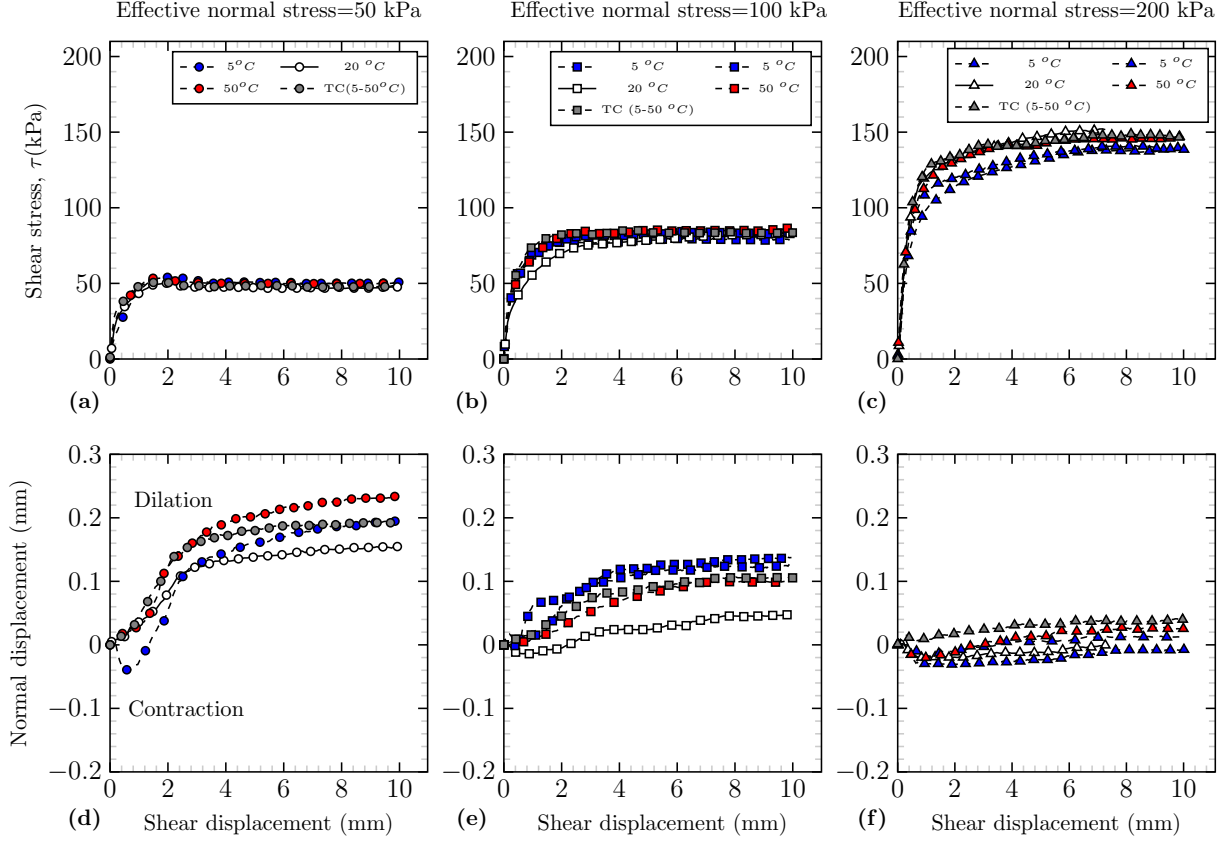


Figure 11: Effect of temperature on shear stress and normal displacement at three different effective normal stresses a-d) 50 kPa b-e) 100 kPa and c-f) 200 kPa, TC=temperature cycles.

Table 5: Shear characteristics of studied soil for different temperatures.

T (°C)	$\tau$ (kPa)			c (kPa)	$\varphi$ (°)
	$\sigma'_n=50$ kPa	$\sigma'_n=100$ kPa	$\sigma'_n=200$ kPa		
5	49.7	79.0	137.0	20.6	30.5
20	48.0	80.5	150.5	13.0	34.4
50	49.8	84.7	149.5	17.4	33.5
TC(5-50)	48.6	83.7	146.0	17.4	33.0

437 increasing the normal stress, this tendency is fading.

#### 438 4.2.2 Cyclic thermo-mechanical direct shear results

439 For thermal cyclic tests after saturation, the same normal stresses as monotonic section  
 440 ( $\sigma'_n=50, 100,$  and  $200$  kPa) were applied. After reaching the desired normal stress, the  
 441 compacted soil samples were subjected to temperature cycles: they were first heated up  
 442 from  $20$  to  $50$  °C then cooled down from  $50$  to  $5$  °C and subsequently followed by 4  
 443 temperature cycles from  $5$  to  $50$  °C.

444 Figure 10b, c, and d show the volumetric deformation due to the temperature cycles



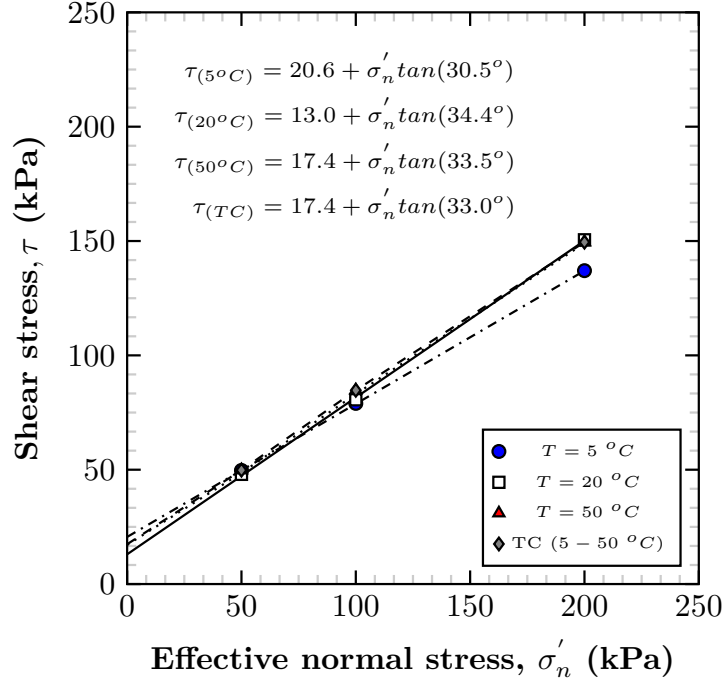


Figure 12: Shear stress against effective normal stress at  $T = 5\text{ }^{\circ}\text{C}$ ,  $T = 20\text{ }^{\circ}\text{C}$ ,  $T = 50\text{ }^{\circ}\text{C}$  and after 5 TC (temperature cycles, 5-50  $^{\circ}\text{C}$ ).

445 under each normal stress. The compacted soil upon heating from 20 to 50  $^{\circ}\text{C}$  contracted  
446 by 0.05, 0.11, and 0.14 % under normal stress of 50, 100, and 200 kPa respectively.  
447 This order of magnitude is coherent with the results of monotonic thermo-mechanical  
448 paths as is shown in Figure 10a. After that, the samples cooled down to 5  $^{\circ}\text{C}$  and  
449 slightly contracted. The contraction of the sample upon the first heating was found to be  
450 irreversible. The first cycle caused a higher contraction compared to subsequent cycles  
451 (Figure 10b, c, and d). The final thermal contractions after 5 thermal cycles were 0.16 %,  
452 0.21 % and 0.22 % under 50, 100 and 200 kPa respectively. When the thermal volumetric  
453 deformation stabilized, the samples were sheared (0.02  $\text{mm}/\text{min}$ ) at 20  $^{\circ}\text{C}$  (Figure 11).  
454 The shear stress corresponding to 10 % of the sample length in table 5 showed that the  
455 temperature cycles have slightly increased the shear strength of the compacted soil under  
456 normal stresses of 50 and 100 kPa while it decreased slightly under 200 kPa compared to  
457 reference tests at 20  $^{\circ}\text{C}$ . This shear stress variation as well as the volumetric response of  
458 the cyclic tests follows the same trend as the monotonic tests at 50  $^{\circ}\text{C}$  (Figure 11). In both  
459 tests, with increasing the normal stress, the dilative response under lower normal stress  
460 (50 and 100 kPa) tends towards a contractive one under higher vertical stress (200 kPa).

461 The Mohr-Coulomb plane after temperature cycles showed that the cohesion increased  
462 by 4 kPa (from 13.0 to 17.4 kPa) and the friction angle remained unchanged compared  
463 to the reference test at 20 °C (Table 5). The variation of the cohesion was the same as  
464 the test at 50 °C. If the volumetric deformation due to heating will be one reason for the  
465 shear increase, it can be concluded that the first heating has a significant impact on the  
466 shearing response.

## 467 5 Discussion

### 468 5.1 Temperature effect on consolidation parameters

469 The shrinkage of the elastic domain, generally denoted thermal softening in literature,  
470 is generally explained by the temperature-dependent properties of water and changes  
471 in the fabric of pores structure (Baldi et al. 1988; Mon et al. 2013). This thermal  
472 softening causes the normal consolidation line shifts to the left and consequently the  
473 apparent preconsolidation pressure decreases (Tidfors and Sällfors 1989; Shariatmadari  
474 and Saeidijam 2012).”

475 In terms of consolidation behavior, temperature variations had a negligible effect on  
476 the compression index ( $C_c$ ) and swelling index ( $C_s$ ) of the studied compacted soil but they  
477 had an impact on apparent preconsolidation pressure ( $\sigma'_p$ ). The observed results are in  
478 accordance with those of other authors on saturated natural and compacted soil samples  
479 ( François et al. 2007; Kaddouri et al. 2019).

480 The shrinkage of the elastic domain, generally denoted thermal softening in literature,  
481 is generally explained by the temperature-dependent properties of water and changes  
482 in the fabric of pores structure (Baldi et al. 1988; Marques et al. (2004); Mon et al.  
483 2013). This thermal softening causes the normal consolidation line shifts to the left  
484 and consequently the apparent preconsolidation pressure decreases (Marques et al. 2004;  
485 Tidfors and Sällfors 1989; Shariatmadari and Saeidijam 2012).

## 5.2 Volumetric response due to the temperature cycles

The thermo-elastoplastic volumetric response of the compacted soil due to temperature cycles under different vertical stresses was found to be state-dependent (OC or NC). Whatever the vertical stresses, in the overconsolidated state, the elastic volumetric deformation was induced whereas in normally consolidated states, for both oedometric and shear tests, a significant thermal plastic strain was observed during the first temperature cycle (Figures 8 and 10). After the first cycle, subsequent cycles induced lower thermal plastic strain. In NC state, the sample is subjected to the maximum experienced vertical stress, and simultaneously, the temperature is raised. This modification would lead to a decrease in pore water viscosity, which consequently increases the permeability and facilitates the particle rearrangements. Campanella and Mitchell (1968), Baldi et al. (1988), Di Donna and Laloui (2015); Ng et al. (2019) and Shetty et al. (2019) observed the same type of thermo-plastic strain induced by heating-cooling cycles, in NC clayey and silty clay soils. Some researchers reported that the amount of thermal volumetric change depends on the plasticity index (PI) of the soil (Abuel-Naga et al. 2007; Ghaaowd et al. 2015). The soil with higher plasticity index shows more thermo-plastic deformation (Delage et al. 2000). Di Donna and Laloui (2013) reported a volumetric deformation of 0.6 % for natural silty clay soils with a plasticity index of 18% while, for the studied soil in this paper, the volumetric deformation was 0.15% with a plasticity index of 6.6% .

## 5.3 Temperature cycles effect on consolidation parameters

The compacted soil in NC state after being subjected to thermal cycles (under 170 and 400 kPa), was reloaded vertically at 20 °C. After thermal plastic deformation and void ratio decrease, the compacted soil shows less compressibility with subsequent loading (slope of  $a_c$  is less than the compression index,  $C_c$  at 20 °C, Figure 9b). This behavior can be due to the increase in the stiffness and hardness of the soil caused by thermal cycles. While by subsequent loading the void ratio converged to the void ratio of the reference oedometric test at 20 °C (Figure 9b and 9c). This means that the impact of thermal plastic deformation of the compacted soil in NC state disappears upon subsequent

514 loading. This observation is corroborated with the findings reported by Di Donna and  
515 Laloui (2013) and Shetty et al. (2019) who have studied the effect of thermal cycles on  
516 the thermal volumetric change of silty clay soil.

#### 517 **5.4 Heating or cooling and temperature cycles effect on shear characteristics**

518 In terms of structural stability of an embankment made of studied compacted soil, the  
519 friction angle was not affected by temperature variation which has been confirmed by  
520 several studies on other soils in the literature (Hueckel and Baldi 1990; Burghignoli et al.  
521 2000; Ghahremannejad 2003; Cekerevac and Laloui 2004; Maghsoodi et al. 2020). The  
522 induced thermal volumetric deformation during heating or temperature cycles slightly  
523 increased the cohesion. Cooling decreased the shear stress under higher normal stresses  
524 and consequently, the cohesion increased by 7.6 kPa.

525 In consolidation and shear behavior, two different behavior was observed. Regarding  
526 the consolidation behavior, on one hand, the heated compacted soil showed a softening  
527 behavior, on the other hand, the shear stress slightly increased. The increase in cohesion  
528 can be related to the thermal volumetric contraction that occurred in the heating phase  
529 which densified the samples. At lower temperature ( $5\text{ }^{\circ}\text{C}$ ) oedometric tests showed lower  
530 settlement during the consolidation phase, while, the shear test results showed that the  
531 compacted soil under high normal stress has low shear strength. This trend needs to be  
532 confirmed with triaxial tests or other tests under higher stress. This could be explained  
533 by the fact that the links between soil particles in low temperatures at the microstructural  
534 level could become more fragile and consequently the strength could decrease. Further  
535 investigations on the microstructure of heated and cooled specimens are necessary to  
536 confirm this explanation.

537 Regarding the volumetric response during shearing, the dilatation is the result of two  
538 different events: (i) rolling and sliding of soil particles (ii) normal stress-induced con-  
539 traction. The soil particle rearrangements caused a disturbance and result in a volume  
540 augmentation, whereas the contraction process decreases the soil volume. When the nor-  
541 mal stress is relatively small, the soil particle rolling and the subsequent disorder are

542 dominant. In high normal stresses, the contraction becomes more dominant and the par-  
543 ticle rearrangement is confined (Yavari et al. 2016; Zhao et al. 2017; Kouakou et al. 2020).  
544 Therefore, the dilatation decreases with normal stress increase.

## 545 **5.5 Engineering implications of results**

546 Based on thermo-mechanical paths in this study, it can be confirmed that in the construc-  
547 tion phase the horizontal heat exchanger loops can be placed in different depths in an  
548 embankment. The experimental results showed that the temperature variations, either  
549 monotonic (heating or cooling) or temperature cycles tend towards conservation or even  
550 improvement of bearing capacity and embankment slopes stability. In terms of consoli-  
551 dation behavior in thermal charging and discharging seasons, when the compacted soil is  
552 exposed to monotonic temperature variations, due to the very small differences in com-  
553 pression index at different temperatures, the effect of temperature on the embankment  
554 global settlement can be considered negligible. Furthermore, the volumetric response un-  
555 der different vertical stresses (50 to 200 kPa) at different embankment depths (2.5 to 10  
556 m) due to heating and temperature cycles could be also small enough to be neglected.

557 Thus, it can be concluded that the effect of temperature on the global mechanical  
558 behavior of the studied compacted soil with temperature variation range from 5 to 50  
559 °C could be negligible. It should be noted that the embankment is in interaction with  
560 the atmosphere from its top and lateral surfaces, the thermal efficiency of the structure  
561 could be affected due to the heat losses. Consequently, it is better to place the heat  
562 exchangers far from the top and lateral surfaces. The tests in this study were performed  
563 on compacted soil at an initial optimal compaction state for thermal properties ( $w=16.3$   
564 and  $\rho_d = 1.79Mg.m^{-3}$ ). This initial soil condition could affect thermo-hydro-mechanical  
565 responses to the temperature variation. Therefore, the initial soil compaction state should  
566 take into account the optimal thermal soil properties.

## 6 Conclusions

This study investigated the consolidation and shear behavior of compacted sandy lean clay subjected to the monotonic and cyclic temperature variations. This type of soil is frequently used for embankment application in France. It should be noted that these tests were performed in the saturated state which underestimates soil mechanical properties. The temperature-controlled oedometric and direct-shear devices were used to perform non-isothermal tests.

Based on the results of the oedometric test, the following conclusions can be drawn:

- the heated compacted soil shows a softening behavior, in contrast, cooled compacted soil shows hardening behavior;
- the compression index and swelling index were unchanged with temperature variation;
- the apparent preconsolidation pressure decreased with heating and increased with cooling;
- the volumetric response of compacted soil depends on the stress history. In an over-consolidated state, a reversible deformation was observed, and in a normally consolidated state the temperature cycles induced a thermal plastic contraction;
- the compacted soil subjected to temperature cycles showed a hardening behavior.

The results of direct shear tests showed that heating from 20 to 50 °C and temperature cycles had a negligible effect on shear characteristics whereas cooling from 20 to 5 °C decreased the shear stress at higher normal stresses (200 kPa).

These results are essential in designing the energy geostructures in a similar range of temperatures. Further work should be performed to investigate the microstructural behavior of studied soil due to heating or cooling. Moreover, in terms of thermal efficiency behavior, a numerical simulation will be performed to investigate the suitable position of horizontal heat exchanger loops due to the heat loss caused by soil-atmospheric interaction.

## References

- 593
- 594 Abedin, A. and Rosen, M., 2011. A critical review of thermochemical energy storage  
595 systems, *The open renewable energy journal* **4**(1).
- 596 Abuel-Naga, H., Bergado, D., Bouazza, A. and Ramana, G., 2007. Volume change be-  
597 haviour of saturated clays under drained heating conditions: experimental results and  
598 constitutive modeling, *Canadian Geotechnical Journal* **44**(8): 942–956.
- 599 Abuel-Naga, H., Bergado, D., Soralump, S. and Rujivipat, P., 2005. Thermal consolida-  
600 tion of soft bangkok clay, *Lowland Technology International Journal* **7**(1): 13–22.
- 601 AFNOR, P., 1993. 94–051. soil: investigation and testing–determination of atterberg’s  
602 limits–liquid limit test using casagrande apparatus–plastic limit test on rolled thread,  
603 *Association Française de Normalisation* .
- 604 ASTM, D., 1994. 3080-90: Standard test method for direct shear test of soils under  
605 consolidated drained conditions, *Annual book of ASTM standards* **4**: 290–295.
- 606 ASTM, D., 2011. Standard test methods for one-dimensional consolidation properties of  
607 soils using incremental loading.
- 608 ASTM, E., 2000. 2089-00. standard practices for ground laboratory atomic oxygen inter-  
609 action evaluation of materials for space applications, *Annual book of ASTM standards*  
610 .
- 611 Baldi, G., Hueckel, T. and Pellegrini, R., 1988. Thermal volume changes of the mineral–  
612 water system in low-porosity clay soils, *Canadian geotechnical journal* **25**(4): 807–825.
- 613 Beier, R. A. and Holloway, W. A., 2015. Changes in the thermal performance of horizontal  
614 boreholes with time, *Applied Thermal Engineering* **78**: 1–8.
- 615 Boukelia, A., 2016. *Modélisations physique et numérique des géostructures énergétiques*,  
616 PhD thesis, Université de Lorraine.
- 617 Burghignoli, A., Desideri, A. and Miliziano, S., 2000. A laboratory study on the thermo-  
618 mechanical behaviour of clayey soils, *Canadian Geotechnical Journal* **37**(4): 764–780.

- 619 Campanella, R. G. and Mitchell, J. K., 1968. Influence of temperature variations on soil  
620 behavior, *Journal of Soil Mechanics & Foundations Div.*
- 621 Casagrande, A., 1936. The determination of pre-consolidation load and its practical  
622 significance, *Proc. Int. Conf. Soil Mech. Found. Eng. Cambridge, Mass., 1936*, Vol. 3,  
623 p. 60.
- 624 Cekerevac, C. and Laloui, L., 2004. Experimental study of thermal effects on the mechan-  
625 ical behaviour of a clay, *International journal for numerical and analytical methods in*  
626 *geomechanics* **28**(3): 209–228.
- 627 Delage, P., Sultan, N. and Cui, Y. J., 2000. On the thermal consolidation of boom clay,  
628 *Canadian Geotechnical Journal* **37**(2): 343–354.
- 629 Delage, P., Sultan, N., Cui, Y.-J. and Ling, L. X., 2009. Permeability changes in boom clay  
630 with temperature, *International Conference and Workshop” Impact of Thermo-Hydro-*  
631 *Mechanical-Chemical (THMC) processes on the safety of underground radioactive waste*  
632 *repositories”, European Union, Luxembourg, 29 September-1 October 2009.*
- 633 Di Donna, A., 2014. *Thermo-mechanical aspects of energy piles*, PhD thesis.
- 634 Di Donna, A. and Laloui, L., 2013. Soil response under thermomechanical conditions  
635 imposed by energy geostructures, *Energy Geostructures: Innovation in Underground*  
636 *Engineering* pp. 3–21.
- 637 Di Donna, A. and Laloui, L., 2015. Response of soil subjected to thermal cyclic loading:  
638 experimental and constitutive study, *Engineering Geology* **190**: 65–76.
- 639 Eriksson, L., 1989. Temperature effects on consolidation properties of sulphide clays,  
640 *International Conference on Soil Mechanics and Foundation Engineering: 13/08/1989-*  
641 *18/08/1989*, Balkema Publishers, AA/Taylor & Francis The Netherlands, pp. 2087–  
642 2090.
- 643 François, B., Salager, S., El Youssoufi, M., Ubals Picanyol, D., Laloui, L. and Saix, C.,  
644 2007. Compression tests on a sandy silt at different suction and temperature levels,  
645 *Computer applications in geotechnical engineering*, pp. 1–10.



- 646 Gan, G., 2013. Dynamic thermal modelling of horizontal ground-source heat pumps,  
647 *International Journal of Low-Carbon Technologies* **8**(2): 95–105.
- 648 Ghaaowd, I., Takai, A., Katsumi, T. and McCartney, J. S., 2015. Pore water pressure  
649 prediction for undrained heating of soils, *Environmental Geotechnics* **4**(2): 70–78.
- 650 Ghahremannejad, B., 2003. Thermo-mechanical behaviour of two reconstituted clays.
- 651 Hesaraki, A., Holmberg, S. and Haghghat, F., 2015. Seasonal thermal energy storage  
652 with heat pumps and low temperatures in building projects—a comparative review,  
653 *Renewable and Sustainable Energy Reviews* **43**: 1199–1213.
- 654 Hillel, D., 1980. Fundamentals of soil physics academic, *San Diego, CA* .
- 655 Hueckel, T. and Baldi, G., 1990. Thermoplasticity of saturated clays: experimental  
656 constitutive study, *Journal of geotechnical engineering* **116**(12): 1778–1796.
- 657 Iverson, R. M. and Major, J. J., 1987. Rainfall, ground-water flow, and seasonal movement  
658 at minor creek landslide, northwestern california: Physical interpretation of empirical  
659 relations, *Geological Society of America Bulletin* **99**(4): 579–594.
- 660 Jradi, M., Veje, C. and Jørgensen, B., 2017. Performance analysis of a soil-based thermal  
661 energy storage system using solar-driven air-source heat pump for danish buildings  
662 sector, *Applied Thermal Engineering* **114**: 360–373.
- 663 Kaddouri, Z., Cuisinier, O. and Masrouri, F., 2019. Influence of effective stress and  
664 temperature on the creep behavior of a saturated compacted clayey soil, *Geomechanics  
665 for Energy and the Environment* **17**: 106–114.
- 666 Kouakou, N., Cuisinier, O. and Masrouri, F., 2020. Estimation of the shear strength of  
667 coarse-grained soils with fine particles, *Transportation Geotechnics* **25**: 100407.
- 668 Lahoori, M., Jannot, Y., Rosin-Paumier, S., Boukelia, A. and Masrouri, F., 2020. Mea-  
669 surement of the thermal properties of unsaturated compacted soil by the transfer func-  
670 tion estimation method, *Applied Thermal Engineering* **167**: 114795.

- 671 Lahoori, M., Rosin-Paumier, S., Stoltz, G. and Jannot, Y., 2020. Thermal conductivity  
672 of nonwoven needle-punched geotextiles: effect of stress and moisture, *Geosynthetics*  
673 *International* pp. 1–9.
- 674 Li, Y., Dijkstra, J. and Karstunen, M., 2018. Thermomechanical creep in sensitive clays,  
675 *Journal of Geotechnical and Geoenvironmental Engineering* **144**(11): 04018085.
- 676 Li, Y., Xu, W., Wang, S., Wang, H. and Dai, Y., 2019. Slope stability analysis with  
677 reference to rainfall infiltration in the yongping copper mine, china., *Current Science*  
678 *(00113891)* **116**(4).
- 679 Liu, J., Yang, C., Gan, J., Liu, Y., Wei, L. and Xie, Q., 2017. Stability analysis of  
680 road embankment slope subjected to rainfall considering runoff-unsaturated seepage and  
681 unsaturated fluid–solid coupling, *International Journal of Civil Engineering* **15**(6): 865–  
682 876.
- 683 Ma, Q., Ng, C., Mašín, D. and Zhou, C., 2017. An approach for modelling volume  
684 change of fine-grained soil subjected to thermal cycles, *Canadian Geotechnical Journal*  
685 **54**(6): 896–901.
- 686 Maghsoodi, S., Cuisinier, O. and Masrouri, F., 2020. Thermal effects on mechanical  
687 behaviour of soil–structure interface, *Canadian geotechnical journal* **57**(1): 32–47.
- 688 Marques, M. E. S., Leroueil, S. and Soares de Almeida, M. d. S., 2004. Viscous behaviour  
689 of st-roch-de-l’achigan clay, quebec, *Canadian Geotechnical Journal* **41**(1): 25–38.
- 690 Mon, E. E., Hamamoto, S., Kawamoto, K., Komatsu, T. and Moldrup, P., 2013. Tem-  
691 perature effects on geotechnical properties of kaolin clay: simultaneous measurements  
692 of consolidation characteristics, shear stiffness, and permeability using a modified oe-  
693 dometer, *GSTF International Journal of Geological Sciences (JGS)* **1**(1).
- 694 Morin, R. and Silva, A. J., 1984. The effects of high pressure and high temperature on  
695 some physical properties of ocean sediments, *Journal of Geophysical Research: Solid*  
696 *Earth* **89**(B1): 511–526.

- 697 Moritz, L., 1995. *Geotechnical properties of clay at elevated temperatures*, Vol. 47, Swedish  
698 Geotechnical Institute Linköping, Sweden.
- 699 Ng, C. W. W., Mu, Q. and Zhou, C., 2019. Effects of specimen preparation method on  
700 the volume change of clay under cyclic thermal loads, *Géotechnique* **69**(2): 146–150.
- 701 Ng, C. W. W. and Zhou, C., 2014. Cyclic behaviour of an unsaturated silt at various  
702 suctions and temperatures, *Géotechnique* **64**(9): 709–720.
- 703 Rahardjo, H., Li, X., Toll, D. G. and Leong, E. C., 2001. The effect of antecedent rainfall  
704 on slope stability, *Unsaturated Soil Concepts and Their Application in Geotechnical*  
705 *Practice*, Springer, pp. 371–399.
- 706 Shariatmadari, N. and Saeidijam, S., 2012. The effect of thermal history on thermo-  
707 mechanical behavior of bentonite-sand mixture, *International Journal of Civil Engi-  
708 neering* **10**(2): 162–167.
- 709 Shetty, R., Singh, D. and Ferrari, A., 2019. Volume change characteristics of fine-grained  
710 soils due to sequential thermo-mechanical stresses, *Engineering Geology* **253**: 47–54.
- 711 Stojanović, B. and Akander, J., 2010. Build-up and long-term performance test of a  
712 full-scale solar-assisted heat pump system for residential heating in nordic climatic con-  
713 ditions, *Applied Thermal Engineering* **30**(2-3): 188–195.
- 714 Thibbotuwawa, D. and Weerasekera, K., 2013. Study of stabilization of unstable area  
715 and development of mitigation measures for landslide at peradeniya, due to widening  
716 of town roads, *ENGINEER* **46**(02): 43–57.
- 717 Tidfors, M. and Sällfors, G., 1989. Temperature effect on preconsolidation pressure.
- 718 Uchaipichat, A. and Khalili, N., 2009. Experimental investigation of thermo-hydro-  
719 mechanical behaviour of an unsaturated silt, *Géotechnique* **59**(4): 339–353.
- 720 Yavari, N., 2014. *Aspects géotechniques des pieux de fondation énergétiques*, PhD thesis,  
721 Paris Est.

- 722 Yavari, N., Tang, A. M., Pereira, J.-M. and Hassen, G., 2016. Effect of temperature on the  
723 shear strength of soils and the soil–structure interface, *Canadian Geotechnical Journal*  
724 **53**(7): 1186–1194.
- 725 Yazdani, S., Helwany, S. and Olgun, G., 2019. Influence of temperature on soil–pile  
726 interface shear strength, *Geomechanics for Energy and the Environment* **18**: 69–78.
- 727 Zhao, L., Yang, P., Zhang, L.-C. and Wang, J., 2017. Cyclic direct shear behaviors of  
728 an artificial frozen soil–structure interface under constant normal stress and sub-zero  
729 temperature, *Cold Regions Science and Technology* **133**: 70–81.

## 730 **List of symbols**

- 731 •  $\sigma'_v$  (kPa) Effective vertical stress
- 732 •  $\tau$  (kPa) Shear stress
- 733 •  $\sigma'_n$  (kPa) Effective normal stress
- 734 •  $\sigma'_p$  (kPa) Preconsolidation pressure
- 735 •  $\varphi$  ( $^\circ$ ) Friction angle of soil
- 736 •  $C_c$  (–) Compression index
- 737 •  $C_s$  (–) Swelling index
- 738 •  $c$  (kPa) Cohesion
- 739 •  $T$  ( $^\circ C$ ) Temperature
- 740 •  $w$  (%) water content
- 741 •  $\rho_d$  (Mg/m<sup>3</sup>) Dry density
- 742 •  $e$  (–) void ratio
- 743 •  $\varepsilon_v$  (%) Volumetric deformation
- 744 •  $k$  (m/s) Hydraulic conductivity
- 745 •  $K$  (m<sup>2</sup>) Intrinsic permeability
- 746 •  $\mu$  (Pa.s) Water viscosity
- 747 •  $C_v$  (m<sup>2</sup>.s<sup>-1</sup>) Coefficient of consolidation
- 748 •  $m_v$  (kPa<sup>-1</sup>) Coefficient of volume compressibility
- 749 •  $\gamma_w$  (kN.m<sup>-3</sup>) unit weight of water
- 750 •  $OCR$  Overconsolidated ratio
- 751 •  $NC$  Normally consolidated state
- 752 •  $OC$  Overconsolidated state

753